Numerical modeling of elastic wave scattering by near-surface heterogeneities

Abdulaziz AlMuhaidib and M. Nafi Toksöz, Earth Resources Laboratory, MIT*

SUMMARY

A perturbation method for elastic waves and numerical forward modeling are used to calculate the effects of seismic wave scattering from arbitrary shape shallow subsurface heterogeneities. Wave propagation is simulated using elastic finite difference for several earth models with different near-surface characteristics. The near-surface scattered wavefield is modeled by separating the incident wavefield from the total wavefield by means of a perturbation method. We show that the scattered field is equivalent to the radiation field of an equivalent elastic source excited at the scatterer locations. The scattered waves consist mostly of body waves scattered to surface waves and are, generally, as large as, or larger than, the reflections. The results indicate that the scattered energy depends strongly on the properties of the shallow scatterers and increases with increasing impedance contrast, increasing size of the scatterers relative to the incident wavelength, and decreasing depth of the scatterers. Also, sources deployed at depth generate weaker surface waves, whereas deep receivers record weaker surface and scattered body-to-surface waves.

INTRODUCTION

In land seismic data acquisition, most of the seismic energy is scattered in the shallow subsurface layers by near-surface heterogeneities (e.g., wadis, large escarpments, dry river beds and karst features) that are common in many arid regions such as the Arabian Peninsula and North Africa (Al-Husseini et al., 1981). When surface irregularities or volume heterogeneities are present (Figure 1), the data are contaminated with scattered surface-to-surface and body-to-surface waves, also know as scattered Rayleigh waves or ground roll. These unwanted coherent noise features can obscure weak body wave reflections from deeper structures. Direct surface (Rayleigh) wave scattering has been studied in more detail since the beginning of reflection seismology. However, much less has been done on the effects of near-surface heterogeneities on the up-coming reflections.

The scattered waves are usually neglected in most conventional imaging and interpretation schemes under simplified assumptions of the earth model (e.g., acoustic). They can greatly affect amplitude critical steps like AVO. Scattering effects can be studied by forward modeling to simulate the interactions between different wave phenomena caused by near-surface heterogeneities. The models can also provide insights for developing new processing algorithms to suppress the noise and to enhance the signal-to-noise ratio. Several previous studies have formulated and examined solutions of the forward (Hudson, 1977; Wu and Aki, 1985; Sato and Fehler, 1998) and inverse (Blonk et al., 1995; Herman et al., 2000; Campman et al., 2006) elastic scattering problems for modeling and imaging based on the perturbation method and single-scattering (Born) approximation. These methods have limitations when dealing with large and high-contrast heterogenities. Numerical forward modeling of elastic waves, as opposed to analytical methods, can handle irregular features, large contrast in material properties, and can generate synthetic seismograms that are accurate over a wide range of scatterer properties.

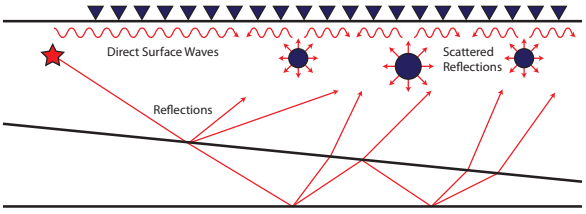

Figure 1: Schematic earth model showing how most of the seismic energy is scattered in the shallow subsurface layers.

In this paper, we utilize an accurate implementation of the standard staggered-grid (SSG) finite-difference scheme that is fourth order accurate in space and second order accurate in time (Virieux, 1986; Levander, 1988; Zhang, 2010). We have computed numerical simulations in two-dimensions for earth models with near-surface scatterers to analyze and assess the effects of scattering mechanisms on recorded seismic waveforms. The perturbation method for elastic waves is used to separate the scattered wavefield from the total wavefield based on a perturbation of the wave equation with respect to medium parameters. Extensive calculations are carried out to study the effects of the acquisition geometry (e.g., source and receiver depths) and the elastic properties of shallow subsurface scatterers (e.g., size, depth, and impedance contrast) on the near-surface scattered wavefield.

MODELING OF ELASTIC WAVE SCATTERING BY NEAR-SURFACE HETEROGENEITIES

In this section, we present the mathematical approach to explain elastic wave scattering using the perturbation method. The general wave equation for an elastic isotropic medium is

$$\rho \frac{\partial^2 u}{\partial t^2} - (\lambda + 2\mu)\nabla(\nabla \cdot \mathbf{u}) + \mu \nabla \times (\nabla \times \mathbf{u}) = 0. \qquad (1)$$

The medium is described by three parameters: the Lame' constants $\lambda(x)$ and $\mu(x)$, and density $\rho(x)$. Seismic P- and S-wave velocities are $c_p = \sqrt{(\lambda + 2\mu)/\rho}$ and $c_s = \sqrt{\mu/\rho}$. The perturbation theory decomposes the medium parameters into background and perturbation parts

$$\begin{aligned} \rho(x) &= \rho_0 + \delta\rho(x) \\ \lambda(x) &= \lambda_0 + \delta\lambda(x) \\ \mu(x) &= \mu_0 + \delta\mu(x). \end{aligned} \qquad (2)$$

We denote by δ and subscript 0 the perturbed and background (reference) medium parameters, respectively. The wavefield in

the background medium is u_0, and it satisfies the elastic wave equation

$$\rho_0 \frac{\partial^2 u_0}{\partial t^2} - (\lambda_0 + 2\mu_0)\nabla(\nabla \cdot \mathbf{u}_0) + \mu_0 \nabla \times (\nabla \times \mathbf{u}_0) = 0. \quad (3)$$

We consider the total wavefield u in the heterogeneous medium as two parts: the incident wavefield u_0 in the background medium, which is the wavefield in the absence of scatterers; and the scattered wavefield $\acute{u}$, which is the difference between the total and incident wavefields:

$$\acute{u}(x) = u(x) - u_0(x). \quad (4)$$

The definition of the perturbation quantities leads to the derivation of a wave equation for the scattered wavefield $\acute{u}$. By subtracting (3) from (1) we obtain

$$\rho_0 \frac{\partial^2 \acute{u}}{\partial t^2} - (\lambda_0 + 2\mu_0)\nabla(\nabla \cdot \acute{\mathbf{u}}) + \mu_0 \nabla \times (\nabla \times \acute{\mathbf{u}})$$
$$= -\left[\delta\rho \frac{\partial^2 u}{\partial t^2} - (\delta\lambda + 2\delta\mu)\nabla(\nabla \cdot \mathbf{u}) + \delta\mu \nabla \times (\nabla \times \mathbf{u})\right]. \quad (5)$$

The left-hand side of equation (5) describes wavefield scattering in the background medium (e.g., reference medium parameters) that includes multiply-scattered waves. The right-hand side is equivalent to an elastic source term that depends on the perturbations of the medium parameters, and the Green's function of the total wavefield (e.g., in the heterogeneous medium). At this point, we show that it is equivalent to obtain the scattered wavefield by either solving equation (5) directly based on the perturbation method (Wu, 1989) or by solving equations (1) and (3) independently numerically using finite difference and then subtracting the incident from the total wavefield. In this paper, we follow the later approach.

APPLICATIONS TO THE EARTH MODEL WITH NEAR-SURFACE HETEROGENEITIES

To study the effects of near-surface heterogeneities on the recorded waveforms, we consider a simple earth model with a single layer over half-space and two circular scatterers embedded in the shallow layer (Figure 2). The two scatterers are located at (x, z) = (360 m, 15 m) and (x, z) = (720 m, 15 m), each has 20 m diameter and an impedance contrast corresponding to 0.36. The P-wave, S-wave and density values of the first layer are 1800 m/s, 1000 m/s and 1750 kg/m^3 and for the half-space and scatterers are 3000 m/s, 1500 m/s and 2250 kg/m^3, respectively. The domain has N_x = 1001 and N_z = 501 grid points with 1 m grid spacing (i.e., Δx and Δz). The time step is 0.2 ms. An explosive point source is used with a Ricker wavelet and 30 Hz dominant frequency. The source is located at (x, z) = (150 m, 10 m). The receivers are located on the surface with 50 m near-offset and 5 m space intervals. In this paper, we consider only the vertical component of the particle velocity field (v_z).

Snapshots of the total and scattered wavefields that are governed by equations (1) and (5) are shown in Figures 4(a) and 4(b), respectively. Note that we do not show the scattered surface-to-surface waves in the scattered wavefield figure because they are much larger in amplitude compared to the scattered body-to-surface waves. The removal of the direct surface (Rayleigh) waves is achieved by first computing the wavefield for a homogeneous full-space with and without the scatterers. Then, we subtract the direct surface waves from the incident and total wavefields to look only at scattered body waves. The upcoming body P- and S-wave reflections, including multiples, impinge on the near-surface heterogeneities and scatter to weak P- and S- waves, acting as secondary sources. Because the scatterers, which are at 15 m depth, are shallower than 1/3 of the wavelength ($\lambda_p = 60$ m), the body wave reflections (incident wavefield) scatter to strong surface waves. These wave features are also shown in the shot-gathers in Figure 3. The scattered waves are comparable in amplitude to the incident reflected signal. A few of these scatterers that are close to the free-surface could mask the primary reflections by the scattered body-to-surface waves. In all the cases we studied in this paper (except for the receiver depth analysis in which we use a vertical source at the surface), we consider a point source at 10 m depth to minimize surface wave energy relative to body wave reflections.

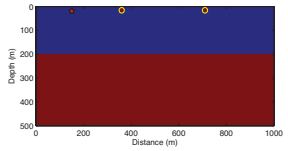

Figure 2: An earth model with a single layer over half-space and two circular scatterers embedded in the shallow layer. The source location is indicated by the red star.

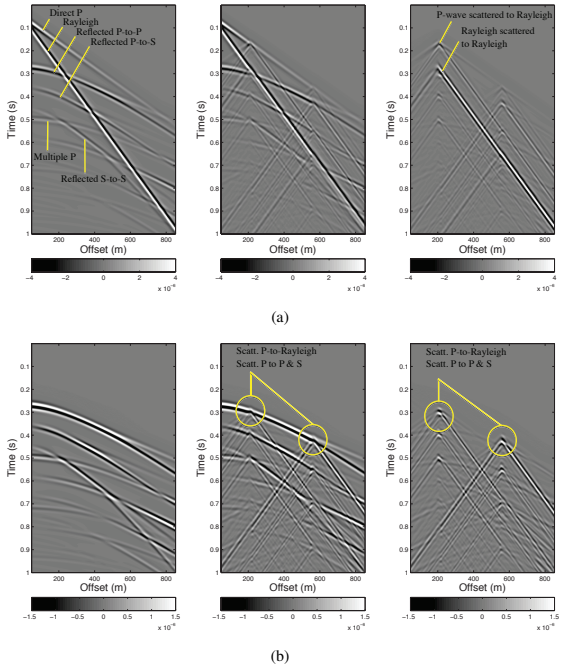

Figure 3: Finite-difference simulations for the model in Figure 2 showing the incident wavefield (left), total wavefield (middle), and scattered wavefield (right); (a) including the direct surface-wave, and (b) with the direct surface wave removed. Note the complexity due to scattering of the reflected arrivals.

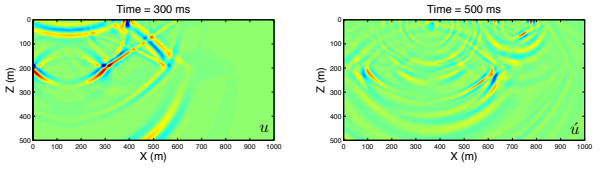

(a) (b)

Figure 4: Snapshots of the wavefield for the model in Figure 2; (a) the total (u) wavefield at 300 ms, and (b) the scattered wavefield $(\acute{u})$ at 500 ms.

Effects of source and receiver depths

The seismic source and receiver depths have significant impact on the recorded waveforms, especially on the strength of the surface (Rayleigh) wave energy. To quantitatively assess the influence of near-surface heterogenities, we assume that scattered waves are noise and calculate the signal-to-noise ratio (SNR) in decibels (dB) for different source and receiver configurations. Seismic sources deployed at depth can minimize the energy of direct surface-wave and, therefore, improve the SNR in the seismic records as the amplitude of surface waves decays exponentially with depth (Figure 5(a)). However, source depths have no effects on the scattered body-to-surface waves, mainly because scattered waves are excited by the near-surface heterogeneities and is independent of the seismic source depth (Figure 5(b)). On the other hand, deploying receivers at depth can improve the SNR as they sample the weaker energy of both the direct and scattered surface waves (Figures 5(c) and 5(d)).

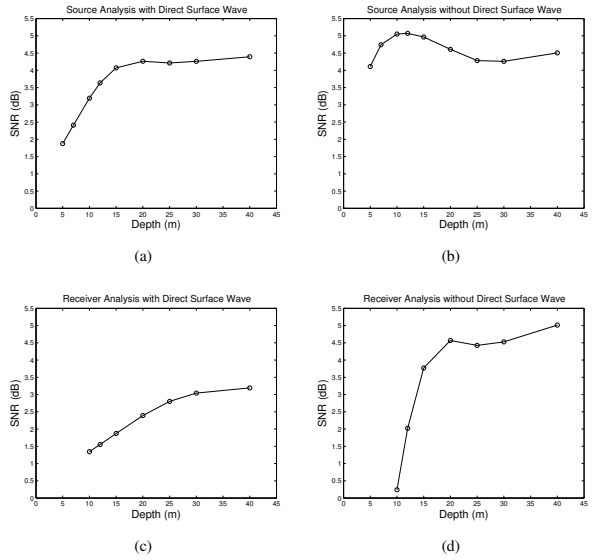

(a) (b)

(c) (d)

Figure 5: The effects of source and receiver depths on the SNR due to shallow scatterers; (a-b) sources, and (c-d) receivers.

Effects of scatterers' depth, size, and impedance contrast

As discussed in the previous section, the seismic source and receiver depths have great effects on the recorded signal. Nevertheless, the characteristics of near-surface scatterers (e.g., impedance contrast, depth, and size) have similar, if not even greater, effects. We quantitatively assess the effects of these factors by calculating the SNRs. The aim is to understand when the scattered waves have significant impact on the quality of the recorded data. The results of different simulations with varying properties are summarized in Figures 6 and 7 as expressed by SNRs. The results indicate that the scattering energy increases with increasing impedance contrast, increasing size of the scatterers relative to the source wavelength, and decreasing depth of the scatterers. As discussed in the previous section, deeper receivers improve the SNR as they record weaker direct and scattered surface waves, whereas deeper sources improve the SNR only because they excite weaker direct surface waves. The same relationships hold for different impedance contrast (Figures 6a and 7a, d) and sizes of scatterers (Figures 6c and 6c, f). Note, however, that deeper source has no effect on the scattered body-to-surface waves as indicated by the narrow range of SNR values for different source depths in Figure 6d-f. These relations hold only when the heterogeneities are shallow (e.g, 15 m depth) and excite significant scattered surface wave energy. In the case where the scatterers are close to the free surface, the scattered energy is dominated by body-to-surface wave scattering. When the scatterers are deeper than $1/3$ of the wavelength (e.g., 20 m), weak or no scattered surface waves are generated.

SCATTERING DUE TO BEDROCK TOPOGRAPHY (INTERFACE SCATTERING)

In the previous sections we showed the examples of scattering from isolated individual scatterers. Bedrock topography can also cause scattering and could have pronounced effects on the quality of recorded waveforms. We consider a synthetic earth model with an irregular (Gaussian) bedrock surface below a homogeneous surface layer, as shown in Figure 8. The P-wave, S-wave and density values for the first layer are 1800 m/s, 1000 m/s and 1750 kg/m^3, for the second layer are 3000 m/s, 1500 m/s and 2250 kg/m^3, and for the half-space are 5000 m/s, 2250 m/s and 2750 kg/m^3, respectively. An explosive point source at 10 m depth is used with a Ricker wavelet and 30 Hz central frequency. The receivers are located on the surface with 50 m near offset and 5 m space intervals. Simulated waveforms recorded at surface for bedrock interface at 15 m and 45 m depths are shown in Figures 9(a) and 9(b), respectively.

The influence of the irregular bedrock interface is clearly demonstrated, as it acts as a continuous line of sources with diffusive-type scattering. At 15 m interface depth, we observe a strong surface wave dispersion due to the thin layer (Figure 9(a)). Because the Rayleigh wave amplitude at a depth deeper than one wavelength ($\lambda_R \sim 31$ m) is very small, both scattering and dispersion of surface waves are very minimal for the interface at 45 m depth (Figure 9(b)). The irregular interface also causes the up-going reflections and refracted waves to scatter to P- and S-waves. When the irregular interface is shallow, up-going body waves and refracted waves that travel along the irregular interface boundary scatter to surface waves. The energy of scattered surface waves decreases as the depth of the bedrock interface increases, mainly because the bedrock acts

as a source of scattered waves. The scattering energy is dominated by body-to-body waves (e.g., relatively weak) for deep scatterers. However, scattering of body and refracted waves to surface waves (e.g., relatively strong) is dominated for the shallow irregular interface.

CONCLUSION

We have presented a numerical approach for modeling elastic wave scattering that can be applied to a general case of an arbitrary shape of the scatterer. We show analytically and numerically that the scatterers act as secondary sources for the scattered elastic wavefield. We have carried out extensive numerical experiments to study the effects of scattered surface waves on SNR. The results show that scattering of up-going reflections by the heterogeneities to surface waves is significant. The scattered energy increases with increasing impedance contrast and increasing size of the scatterers relative to the incident wavelength. Scattering decreases with increasing depth of scatterers. Additionally, the strength of the generated surface (Rayleigh) waves also depends on the source depth. Sources located at depths below 1/3 of the wavelength excite weaker surface waves and, therefore, improve the SNR due to Rayleigh wave scattering. However, source depth does not affect the scattering of reflected body waves. On the other hand, receivers deployed at depths below 1/3 of the wavelength improve the SNR as they sample the weak part of the direct and scattered surface waves.

ACKNOWLEDGMENTS

We thank Saudi Aramco and ERL founding members for supporting this research.

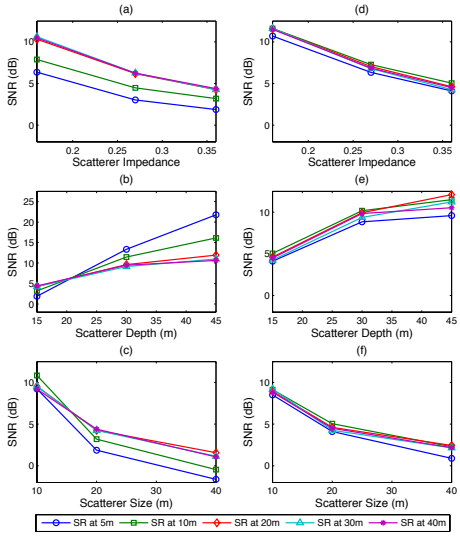

Figure 6: The effects of source depths on the SNR due to characteristics of near-surface heterogeneities (impedance contrast, depth, and size), (a-c) including the direct surface-wave, and (d-f) with the direct surface-wave removed.

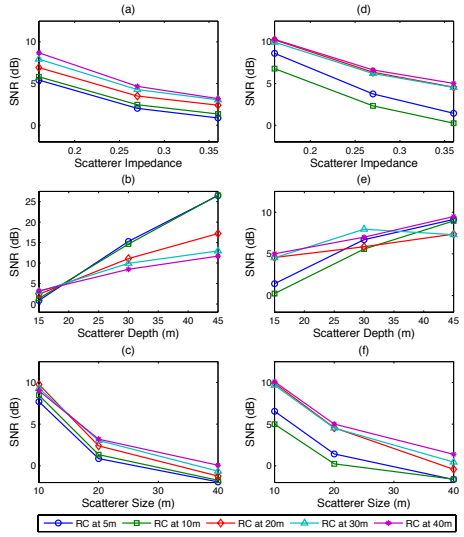

Figure 7: The effects of receiver depths on the SNR due to characteristics of near-surface heterogeneities (impedance contrast, depth, and size), (a-c) including the direct surface-wave, and (d-f) with the direct surface-wave removed.

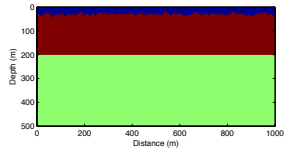

Figure 8: An earth model with near-surface irregular (Gaussian) bedrock interface and deeper plane reflector.

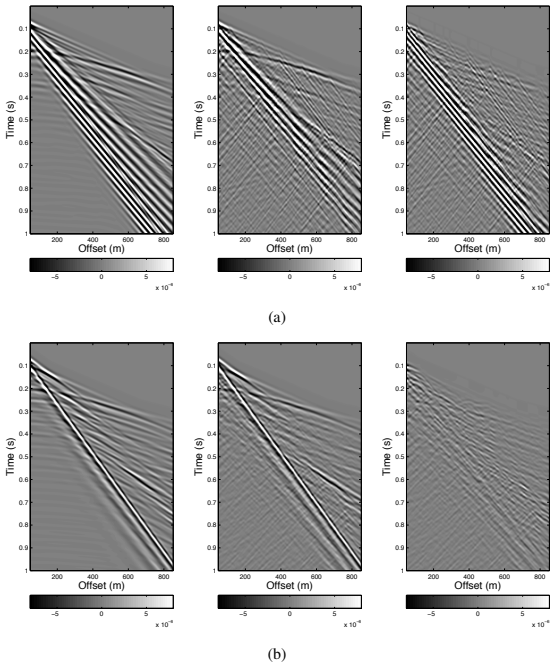

Figure 9: Simulations for the shallow interface at (a) 15 m, and (b) 45 m depth; (left) incident wavefield (plane interface); (middle) total wavefield; and (right) scattered wavefield.